

# Influence of unlike dispersion interactions in modeling methane clathrate hydrates

Matthew Lasich,<sup>a</sup> Amir Hossein Mohammadi,<sup>a</sup> Kim Bolton,<sup>b</sup> Jadran Vrabc,<sup>c</sup> and Deresh Ramjugernath<sup>a,\*</sup>

<sup>a</sup> *Thermodynamics Research Unit, University of KwaZulu-Natal, Durban 4041, South Africa*

<sup>b</sup> *School of Engineering, University of Borås, Borås 501 90, Sweden*

<sup>c</sup> *Thermodynamik und Energietechnik, University of Paderborn, Paderborn 33098, Germany*

\* Corresponding author. E-mail address: [Ramjuger@ukzn.ac.za](mailto:Ramjuger@ukzn.ac.za)

## Abstract

Studies of the thermodynamic stability of clathrate hydrates of natural gas (mostly methane) is important in fields such as offshore gas exploitation and energy storage. Two approaches were used to study the effect of unlike dispersion interactions on methane clathrate hydrates: grand canonical Monte Carlo simulations (which yield adsorption data directly and can be used to infer phase equilibria), and estimation of the heat of dissociation coupled with the Clausius-Clapeyron equation (to calculate the phase equilibria, at the expense of providing no information about the adsorption behaviour). It was found that the adsorption isotherm parameters change monotonically with respect to unlike dispersion interactions, although a perfect fit to experimentally-derived values may not be possible, at least using the force fields considered in this study. The heat of dissociation changes monotonically due to changes in the unlike dispersion interaction, and a best fit value of the Berthelot correction factor is achieved.

**Keywords:** Clathrate hydrate; Combining rule; Dispersion

## 1. Introduction

Clathrate hydrates resemble ice, and form from a gas species trapped within a network of hydrogen-bonded water molecules. Naturally occurring clathrate hydrates contain primarily methane as the guest molecule, and are found in the deep ocean or permafrost [1]. Methane hydrates are a major concern in offshore operations [2], as it frequently forms blockages in natural gas pipelines [3]. However, methane hydrates are also of interest as an energy storage medium due to the relatively low cost of the storage material, which is essentially water [4,5].

The effect of unlike dispersion interactions on adsorption in methane clathrate hydrates has not yet been studied in detail, although such a study has recently been undertaken for argon clathrate hydrates [6]. The effects of dipole moment, molecular size, and other parameters on the stability of clathrate hydrates have been studied by laboratory experiments [7,8]. However, such experiments do not allow for full control of molecular parameters, which is possible with molecular computations. By varying the molecular properties, the physical mechanisms of guest molecule adsorption can be studied directly.

The standard Lorentz [9] and Berthelot [10] combining rules are commonly used for specifying the parameters of unlike Lennard-Jones (LJ) interactions [11] between different molecule types [12]. However, their applicability to systems containing nonpolar and polar molecules may not be optimal. For instance, gas-water interactions are not well described by these combining rules [13]. Extensive discussions on the general use of combining rules can be found in the literature [6,13-17], although there is little work with respect to clathrate hydrates. The use of the standard Lorentz and Berthelot rules for clathrate hydrate systems has only recently been discussed in the literature [18].

An extensive study was performed recently to determine the effects of the Lorentz and Berthelot combining rules on adsorption in argon clathrate hydrates [6]. Changes in the Lorentz and Berthelot combining rules resulted in significant changes in adsorption for the sII and sH clathrate hydrate structures, due to the size differential between the cages present in these structures. The effects were considered to be weak for the sI argon clathrate hydrate. It

should also be noted, however, that the LJ parameters of argon were adjusted, and not the unlike interactions between argon and water.

The study focuses on the Berthelot rule, since previous studies [18—20] have shown that for spherical (e.g., argon) or approximately spherical molecules (e.g., methane), an additional ‘polarizability’ contribution to the guest-water interactions must be considered. This is achieved in a computationally expedient way [18] through the introduction of a correction factor to the Berthelot rule. The polarizability contribution is purely a dispersion/energetic effect, and so the size parameter remains unaffected.

## 2. Theory and methods

### 2.1. Clathrate hydrate phase equilibria

Phase equilibria of clathrate hydrates are described using the van der Waals-Platteeuw theory [21]. The phase equilibrium criterion is the equality of the chemical potential of water in the hydrate and liquid phases, each relative to the hypothetical empty hydrate ( $\Delta\mu_W^H$  and  $\Delta\mu_W^L$ , respectively). Calculation of each of these terms can be achieved by [22]:

$$\Delta\mu_W^H = -R \cdot T \cdot \sum_j [ v_j \ln ( 1 - \sum_i \theta_{ij} ) ] \quad (1)$$

$$\Delta\mu_W^L = R \cdot T \cdot [ \Delta\mu^0 / ( R \cdot T_R ) - T_R \int^T \Delta H_W / ( R \cdot T^2 ) \cdot dT + \int_0^P \Delta V_W / ( R \cdot T ) \cdot dP ] \quad (2)$$

where the indices  $i$  and  $j$  refer to the gas species and cavity type, respectively,  $v_j$  is the ratio of water molecules per unit cell to cavity type  $j$ ,  $\theta_{ij}$  is the fractional occupancy of cavity type  $j$  by gas species  $i$ ,  $\Delta\mu^0$  is  $\Delta\mu_W^H$  at  $T_R = 273.15$  K and  $P_R = 0$  MPa (i.e., the reference state), and  $\Delta H_W$  and  $\Delta V_W$  are the differences in enthalpy and molar volume, respectively, between liquid water and the hypothetical empty hydrate in the reference state. Therefore, once the dependence of the fractional occupancy on temperature and pressure is known, phase equilibria can be estimated using the above relationships.

The fractional occupancy,  $\theta$ , is the number of adsorbed methane molecules per unit cell divided by the total number of adsorption sites per unit cell,  $N/N_T$ , and is calculated by using the Langmuir adsorption constant  $C$  and the fugacity of the gas species  $f$ :

$$\theta = C \cdot f / ( 1 + C \cdot f ) \quad (3)$$

Pressure can be substituted for fugacity in eq. (3), since the deviation is not great [23] over the range of experimental data [24,25] for methane clathrate hydrates. A temperature dependence relationship for the Langmuir adsorption constant [26] was fitted [27] to the simulated adsorption isotherms using two parameters  $A$  and  $B$ :

$$C = (A / T) \cdot \exp ( B / T ) \quad (4)$$

In order to estimate the phase equilibria, eq. (4) can be combined with eqs. (1) through (3).

It was recently found [28,29] that in order to accurately simulate hydrates under equilibrium, the water force field should reproduce the experimental value for the melting point of ice  $I_h$ . However, GCMC simulations assume a priori that the hydrate structure is stable under the conditions considered, and moreover, phase equilibrium is not simulated directly using GCMC simulations. GCMC simulations only consider the phenomenon of adsorption into a stable clathrate lattice, and so can only directly provide information on the loading behaviour of clathrate hydrates. Once the loading behaviour is known, the influence of pressure and temperature on occupancy can be ascertained. Since van der Waals-Platteeuw theory [21] can be used to express the chemical potential of the hydrate phase using the occupancy, the dissociation pressure can then be estimated using adsorption isotherms fitted to experimental data [30]. Thus, the phase equilibria are inferred using the pressure- and temperature-dependence of the occupancies.

By expressing the natural logarithm of the dissociation pressure as a function of the reciprocal of temperature, the heat of dissociation ( $\Delta H_{Diss.}$ ) can be related to the slope of the dissociation pressure curve by the Clausius-Clapeyron equation [31]:

$$d \ln P / d(1 / T) = - \Delta H_{Diss.} / (Z \cdot R) \quad (5)$$

where  $Z$  is the compressibility factor of methane. Methane was considered as an ideal gas when employing eq. (5) in this study, since over the range of experimental temperature and pressure values, the deviation from ideality is not significant [23]. In the case of using GCMC simulations (the first approach considered in this study), the heat of dissociation can only be inferred by examining the effect of adsorption isotherm parameters on the slope of the

dissociation pressure curve. In the second approach in this study, the heat of dissociation itself was estimated directly by computing the enthalpies of the hydrate phase, gaseous methane, and liquid water. These calculated values were subsequently used in the integrated form of eq. (5) to determine the dissociation pressure curve.

## 2.2. Intermolecular interactions

The LJ potential is frequently used to describe intermolecular interactions [30]. In this work, the adsorption isotherms and the heat of dissociation of methane clathrate hydrate were studied directly for different values of the unlike LJ well depth,  $\varepsilon_{ij}$ . This was achieved through application of a binary correction factor,  $k_{ij}$ , to the Berthelot rule:

$$\varepsilon_{ij} = k_{ij} \cdot (\varepsilon_{ii} \cdot \varepsilon_{jj})^{0.5} \quad (6)$$

where  $\varepsilon_{ii}$  and  $\varepsilon_{jj}$  are for the intermolecular interactions between like LJ sites. The reference case is  $k_{ij} = 1.0$  (i.e., the Berthelot rule). It should be noted that that  $\varepsilon_{ij}$  (and by extension,  $k_{ij}$ ) values fitted to data for clathrate hydrate systems are limited in their application to other data for bulk systems [33]. Moreover, molecular interaction parameters fitted to clathrate hydrate data do not match those obtained by fitting to, for example, second virial coefficient, gas viscosity, or molecular beam scattering data [34]. This problem has been discussed in further detail and at great length in the literature [35-46].

It can be noted that the Berthelot rule is a special case of a more general formulation by Reed [47] and extended upon by Hudson and McCoubrey [48], which makes use of both the molecular size parameters and ionization potentials when calculating  $\varepsilon_{ij}$ . The Berthelot rule is returned from the Hudson and McCoubrey rule when the two molecules possess similar sizes and ionization potentials. Therefore, it is not surprising that the unmodified Berthelot rule may be insufficient to describe interactions between methane and water in clathrate hydrate systems [49].

The LJ parameters ( $\varepsilon_{ii}/k_B = 145.27$  K and  $\sigma_{ii} = 0.3821$  nm) of the united atom (UA) methane were calculated [50] from the critical properties [51], and the Simple Point Charge (SPC) water force field [52] was chosen since it has successfully been used in describing clathrate hydrates (albeit without directly considering phase equilibria) [27,53]. Since the

structure-forming properties of water systems obtained from simulations using different force fields are similar [54], and since methane force field parameters are not significantly different [18], it is expected that trends observed in this study should be similar for other force field combinations. Ewald summation [55] was used for the long-range electrostatic interactions up to a real space cut-off distance of 1 nm, and the LJ interactions were truncated at 1 nm. The force field parameters are shown in Table 1.

### 2.3. Grand canonical Monte Carlo simulations

The General Utility Lattice Program (GULP) [56] was employed to perform grand canonical Monte Carlo (GCMC) computer simulations [57,58], using the Metropolis scheme [59]. The chemical potential values required as input for the grand canonical ensemble simulations were estimated using Monte Carlo (MC) simulations via the computer program “ms2” [60]. For these simulations, the system consisted of 500 methane molecules and the ratio of translation:volume change moves was 98:2 [61]. The system was relaxed for 100 MC cycles, followed by equilibration in two stages (using the NVT ensemble for  $2 \cdot 10^4$  cycles, and then the NPT ensemble for  $5 \cdot 10^4$  cycles).  $3 \cdot 10^5$  cycles were then used for data production, and Widom’s method [62] was employed to estimate the chemical potential using 2000 test particles in every cycle. This procedure was employed previously in conjunction with GCMC simulations [27]. One cycle consists of  $N$  moves, where  $N$  is the number of molecules in the system.

A single GCMC simulation consisted of  $10^7$  MC moves (about  $1.85 \cdot 10^5$  cycles). The first 25 % of moves were needed to reach equilibrium, since the number of adsorbed gas molecules usually began to plateau after the first 10 % of the simulation. The following types of MC moves were considered: translation/rotation, particle creation, and particle destruction. The translation/rotation moves mimic the thermal motion of molecules within the clathrate hydrate. The creation and destruction moves (which were only allowed for the gas particles) were analogues for the adsorption and desorption of gas molecules, respectively. Each type of move had an equal probability of occurrence (i.e. 33 %), with translation/rotation moves being equally split within their 33 %. For the sake of rigor, the water molecules were allowed to move (i.e., undergo translation/rotation). The maximum allowed displacement for the translation move was 0.05 nm while no angular limit was set for rotation moves.

A 1x1x1 sI crystal unit cell consisting of 46 water molecules (with periodic boundary conditions) was used, since previous work done with systems of this size [63,64] showed no effects due to finite size or periodicity in GCMC simulations of clathrate hydrate systems. The crystal structure was taken from a previous computational study [65]. The unit cell parameters for the crystal were:  $a = b = c = 1.20$  nm and  $\alpha = \beta = \gamma = 90^\circ$  [5].

The thermodynamic conditions considered were  $T = \{273.2 \text{ K}, 280 \text{ K}, 300 \text{ K}\}$  and  $P = \{1 \text{ MPa}, 10 \text{ MPa}, 60 \text{ MPa}, 100 \text{ MPa}\}$ . This ensures that all of the temperature and pressure values along the dissociation curve above the ice-point were studied. Gas adsorption was described using a linearized form [66] of the Langmuir [67] adsorption isotherm:

$$(P / N) = (1 / N_T) \cdot P + 1 / (C \cdot N) \quad (7)$$

where  $P$  is the system pressure,  $N$  is the number of gas molecules adsorbed per crystal unit cell,  $C$  is the Langmuir adsorption constant, and  $N_T$  is the total number of possible adsorption sites per crystal unit cell. Thus a plot of  $(P/N)$  versus  $P$  yields a straight line for an ideal Langmuir adsorption isotherm.

The range of  $k_{ij}$  values considered in the GCMC simulations was  $\{0.80, 0.85, 0.95, 1.05, 1.07, 1.10, 1.25\}$ . The results for  $k_{ij} = 1.0$  were taken from the literature [27]. This range includes a ‘best fit’ value of  $k_{ij} = 1.07$  obtained from calculations of the excess chemical potential of dilute methane in water [18]. It also takes into account any weak effects that  $k_{ij}$  may have on adsorption in methane clathrate hydrate, since a previous study showed no significant effects of the unlike dispersion interaction on adsorption over the range  $0.8944 < k_{ij} < 1.0954$  [6].

#### 2.4. Direct estimation of the heat of dissociation

Considering eq. (5), it is apparent that if a reference state is considered, along with a set of specified pressure values (for example), then the temperature corresponding to the desired dissociation pressure can be calculated.

In order to make use of eq. (5), MC simulations were performed using the computer program “ms2” [59] for the fluid phases, in order to estimate the enthalpies of pure liquid

water and gaseous methane at the reference conditions (in this case,  $P = 2.80$  MPa and  $T = 273.7$  K; the experimental data point closest to the ice point of water). For these MC simulations, the parameters were the same as for the simulations used to determine the chemical potential of pure methane (see section 2.3), albeit without any use of Widom's method (since it was unnecessary in this case). The same force fields were used as for the GCMC simulations.

For the hydrate phase, GULP [56] was used to calculate the solid phase enthalpy for each  $k_{ij}$  value. Since the fluid phases were assumed to be pure, due to the low solubility of gaseous methane in water (and low water content of pure methane gas) over the conditions of interest [68], fluid phase simulations were only required for  $k_{ij} = 1.0$ . The starting crystal structure was taken from the literature [65], and the structure was optimized to achieve the lowest energy at constant pressure, following a procedure used in the literature [69].

Once energy of the crystal structure had been minimized, the enthalpy  $H$  was computed using for externally specified pressure  $P$  and cell volume  $V$ , along with the static and vibrational contributions to the internal energy,  $U_{Stat.}$  and  $U_{Vib.}$ , respectively:

$$H = U_{Stat.} + U_{Vib.} + P \cdot V \quad (8)$$

The static contribution to the internal energy was calculated from the force field using the spatial coordinates of the interaction sites. The vibrational contribution was calculated using the vibrational frequencies of the lattice, determined from the Hessian matrix. The vibrational frequencies  $\omega$  were then used to determine  $U_{Vib.}$  [70]:

$$U_{Vib.} = \sum_m \sum_k w_k \cdot (0.5 \cdot \omega + h \cdot \omega / (\exp(h \cdot \omega / (k_B \cdot T)) - 1)) \quad (9)$$

The computation proceeds over  $m$  vibrational modes for each point  $k$  in reciprocal space, using weights  $w_k$ . The summation shown in eq. (9) is an integration over the phonon density of states, with the weights such that their sum is equal to one. To achieve this, the standard Monkhorst-Pack scheme was used [71].  $h$  and  $k_B$  are Planck's and Boltzmann's constants, respectively. For the crystal calculations, the electrostatic charges were included using the Born effective charges [72,73]. It is important to point out that this calculation procedure only applies to the solid hydrate phase, and not to the fluid phases (i.e., gaseous methane and

liquid water). For the fluid phases, a similar procedure was used as for the estimation of the chemical potential of methane gas, as described in section 2.3.

Once the enthalpies are calculated for the fluid phases and the hydrate crystal, the heat of dissociation can be estimated using the following reaction:



The hydration number was set to 5.75 since a completely filled methane clathrate hydrate crystal (i.e.,  $\theta = 1$ ) forms the basis for the solid phase enthalpy calculation (in the fully occupied methane clathrate hydrate crystal there are 46 water molecules to 8 methane molecules). The heat of dissociation was determined from the differences in enthalpy of the combined hydrate phase, the gaseous methane, and liquid water [74].

For the approach discussed in this section,  $k_{ij} = \{1, 1.01, 1.02, 1.025, 1.028, 1.029, 1.03\}$ . This range was selected based on the results of a previous study, which obtained ‘best fit’ values for methane clathrate hydrate of  $1.01 < k_{ij} < 1.03$  [69], depending on whether the lattice constant or a perturbation energy term was considered.

### 3. Results and discussion

#### 3.1. Grand canonical Monte Carlo simulations

Changing the unlike dispersion interactions does not significantly change the linearity of the adsorption isotherms at any of the temperatures investigated. In all cases, the adsorption isotherms are linear ( $R^2 > 0.98$ ) when represented in the form of eq. (7), thus indicating that the use of a single site Langmuir-type behaviour is reasonable for different values of  $k_{ij}$ .

Averaged over all data points in this study, increasing the unlike dispersion interactions resulted in an increased quantity of adsorbed methane relative to the reference state of  $k_{ij} = 1.0$  (about 2.5 % for  $k_{ij} = 1.10$ ). Fig. 1 shows a plot of the occupancy  $\theta$  (see eq. (3)) as a function of pressure at  $T = 273.2$  K for all values of  $k_{ij}$  considered in this study (this was done to show a representative data set, since the significant statistical uncertainties make it difficult to discern trends in the raw data). The results for  $T = \{280, 300\}$  K can be found in the supplementary material. There is a weak effect of deviation from the standard Berthelot

rule (i.e.,  $k_{ij} = 1.0$ ) on the adsorption of methane into the clathrate hydrate lattice, especially when the uncertainties in the results of the simulations are considered. This observation concurs with results for sI argon clathrate hydrate obtained by GCMC simulations [6].

The adsorption isotherm parameters  $A$  and  $B$  (see eq. (4)) fitted to the results of the GCMC simulations are shown in Table 2. There are monotonic trends with respect to both  $A$  and  $B$  (if the absolute average deviations are considered), which suggest that these parameters, instead of the adsorption isotherm simulation data themselves, can be used to determine a ‘best fit’  $k_{ij}$  to parameters determined by regression with experimental phase equilibrium data.  $A$  is more strongly influenced by unlike dispersion interactions than  $B$ .

It can be noted that sampling larger systems may lead to lower statistical uncertainties (this study employed  $1 \times 1 \times 1$  crystal unit cells). However, GCMC simulations of clathrates employing  $2 \times 2 \times 2$  unit cells [6] still encountered sizeable uncertainties (about 2 %, on average, for sI argon clathrate hydrates [6]). This can obscure the presence of any effect of changing the unlike dispersion interaction on gas adsorption in methane clathrate hydrates. However, when considering the adsorption isotherm parameters  $A$  and  $B$ , there are monotonic trends, which appears to be at odds with the small effect observed for the adsorption isotherms themselves. Importantly, the adsorption isotherms were determined directly, whereas the parameters  $A$  and  $B$  were fitted to aggregated sets of adsorption isotherm data, and so may more readily capture trends amongst the simulation results as a whole.

It can also be noted here that there are significant differences in the magnitude of the effect of  $k_{ij}$  on  $A$  and  $B$ . Figs. 2 and 3 clearly illustrate a larger range of possible values for  $A$  as compared to  $B$  over the range of unlike dispersion energies considered in this study. For example, increasing the unlike dispersion interaction by 5 % (i.e.,  $k_{ij} = 1.05$ ) from the base scenario (i.e.,  $k_{ij} = 1$ ) produces an increase of 41.9 % in the value of  $A$ , whilst resulting in no measureable change in  $B$ . This shows that there is a large net effect of the unlike dispersion interaction on the temperature-dependent adsorption behaviour.

The use of a flexible water lattice in this study, while more rigorous than assuming a static crystal structure, results in significantly larger statistical uncertainties (about 4 % on average for the quantity of adsorbed methane), due to the possibility of water molecules occasionally reducing the accessible volume of the cavities within the clathrate lattice, and

thus introducing more uncertainty in the acceptance or rejection of insertion of new methane particles as compared to using a rigid lattice.

An additional point to consider is the solution space of the methane clathrate hydrate phase equilibrium calculation. In other words, what sets of  $A$  and  $B$  values can be fitted to the experimental data, and how do these parameters influence the dissociation pressure curve? To study this, a linearized form of the dissociation pressure curve was considered:

$$\log_{10}(P) = (\text{slope}) \cdot T + (\text{intercept}) \quad (11)$$

The phase equilibria of methane clathrate hydrates over the range of interest are highly linear ( $R^2 > 0.99$ ), and so it is possible to describe the dissociation pressure curve well using only the slope and intercept of eq. (11). Fig. 2 shows the slopes, and Fig. 3 shows the intercepts of the dissociation curves associated with each pair of  $A$  and  $B$  values. While there are trends in terms of  $B$  versus  $A$  for the parameters fitted to the results of GCMC simulations, it is apparent that this trend line would not cut the ‘best’ fit set of  $(A,B)$  values and thus it is not possible to produce a perfect fit to experimental data. The nearest approach to the experimental data (shown by the asterisks in the figures) occurs in the range  $1.05 \leq k_{ij} \leq 1.07$ , which is near the value of  $k_{ij} = 1.07$  obtained previously for the methane-water system [18]. However, the hyperbolic relationship between  $A$  and  $B$  can never satisfy both the slope and intercept values of the experimental data simultaneously.

It can be instructive at this point to consider the closest fit  $k_{ij}$  value obtained thus far in comparison to a value calculated via the general formulation by Reed [47] and extended upon by Hudson and McCoubrey [48]. This comparison can illustrate the necessity of determining a ‘best fit’ value of the correction factor using experimental clathrate hydrate data. The unlike dispersion energy calculated via the Hudson and McCoubrey [48] approach is:

$$\varepsilon_{ij} = [ 2 (I_{ii} I_{jj})^{0.5} / (I_{ii} + I_{jj}) ] [ 2 (\sigma_{ii} \sigma_{jj})^{0.5} / (\sigma_{ii} + \sigma_{jj}) ] (\varepsilon_{ii} \varepsilon_{jj})^{0.5} \quad (12)$$

where  $I$  is the ionization potential of the species concerned. To determine  $k_{ij}$  using eq. (12), the following relationship is used:

$$k_{ij} = \varepsilon_{ij}^{HM} / \varepsilon_{ij}^{LB} \quad (13)$$

where  $\varepsilon_{ij}^{HM}$  and  $\varepsilon_{ij}^{LB}$  are the unlike dispersion interactions calculated using the Hudson-McCoubrey and standard Lorentz-Berthelot approaches, respectively. Using the force field parameters in this study, along with ionization potentials from the literature [75,76],  $k_{ij} = 0.996$ . This is clearly at odds with a value of  $1.05 < k_{ij} < 1.07$  which produces a fit closest to the experimental data. Therefore, it is imperative that fitting be undertaken for clathrate hydrate systems using clathrate hydrate data.

Due to the hyperbolic nature of the trend connecting the values for  $A$  and  $B$  shown in Figs. 2 and 3, a similar intercept to that found in experiments [24,25] is achieved for  $0.80 < k_{ij} < 0.95$ . However, the slope and intercept of the dissociation pressure curve are not achieved simultaneously, and so the calculated phase equilibria cannot match the experimental data. With regard to the interval  $1.10 < k_{ij} < 1.25$ , the same slope can be achieved as was observed for the experimental data, but the intercept does not match the experimental data. In other words,  $A$  is hyperbolically related to  $B$ , and this hyperbole never cuts the slope and intercept isolines relating to the experimental data simultaneously, although it cuts one or the other for  $0.80 < k_{ij} < 0.95$  and  $1.10 < k_{ij} < 1.25$ .

Since the slope of the dissociation pressure curve is related to the heat of dissociation (see eq. (5)), any effects of unlike dispersion interactions can also be examined via Fig. 2. For the range of  $k_{ij}$  values in this study, the unlike dispersion interaction does not significantly influence the heat of dissociation. This is evidenced by the fact that the hyperbolic trend connecting all of the values in Fig. 2 correlates fairly well with the isoline corresponding to a slope of approximately  $0.072 \text{ K}^{-1}$ . Therefore, it may not be possible to fit the heat of dissociation inferred from the results of GCMC simulations using  $k_{ij}$ , at least using the force fields considered in this study.

The observations regarding the behaviour of the adsorption isotherm parameters can be considered in relation to a previous study on the argon clathrate hydrates concerning deviations from the Lorentz and Berthelot combining rules [6]. The fact that there are monotonic trends in both  $A$  and  $B$  with respect to  $k_{ij}$ , coupled with the lack of a similar trend in the adsorption of methane into the clathrate hydrate lattice, suggests that the adsorption isotherms of the methane clathrate hydrate ‘warp’ around the reference state of  $k_{ij} = 1.0$ . In

other words, for a decrease in the unlike dispersion interaction at lower pressures, less adsorption occurred, while at higher pressures, more adsorption occurred (the converse was true for the case of increasing the unlike dispersion interaction). Such behaviour was also observed for the argon clathrate hydrates [6].

In addition to gas adsorption, the relationship between the free energy of the hydrate and the strength of gas-water interactions relative to the water-water interactions should be considered. A thorough study of a variety of hydrates, considering both sI and sII hydrates, showed that if the guest species molecules interact too strongly with the water constituting the hydrate lattice, the hydrogen-bond networks can be disrupted by gas-water interactions [60]. Significantly, the previous study showed that there was a minimum in the residual free energy differences between the hydrate systems with respect to the size parameter,  $\sigma_{ii}$ . In other words, if a gas particle was too small or too large, it would disrupt the water-water interactions that stabilise the clathrate structure. Similarly, the results of the present study show that increasing  $\varepsilon_{ij}$  can also disrupt the water-water interactions, as evidenced by the decrease in thermodynamic stability shown for  $k_{ij} = 1.10$  as compared to  $k_{ij} = 1.05$ . Therefore, while increasing the unlike dispersion interaction can produce a more realistic description of the methane clathrate hydrate, this effect can only be achieved up to a point, beyond which increasing the gas-water interaction strength will disrupt water-water bonding.

In order to ascertain whether free energy effects play a role in the simulated adsorption of methane, additional calculations were done using GULP. Using geometric coordinate data from the GCMC simulations, Gibbs free energy calculations were done at  $T = 280$  K and  $P = 10$  MPa (for the sake of comparison), for  $k_{ij} = \{1, 1.05, 1.07, 1.1\}$ . This set of temperature and pressure values was selected since it lies above the hydrate dissociation line for all values of  $k_{ij}$  considered in this study. The Gibbs free energy,  $G$ , was estimated by first determining the Helmholtz free energy,  $A$ :

$$G = A + P \cdot V \tag{14}$$

$$A = U - T \cdot S \tag{15}$$

where  $S$  is the entropy, which was estimated using the vibrational partition function [70], and the internal energy  $U$  was estimated as before (see section 2.4.). The vibrational contributions

are influenced by temperature, whereas the static (or configurational) contributions are purely due to spatial distributions. Since the clathrate hydrate systems considered possess similar occupancies at  $T = 280$  K and  $P = 10$  MPa (see Fig. A1) and the methane molecules are largely located within the centers of the cavities within the sI crystal structure, the configurational entropy can be considered as approximately equal for all  $k_{ij}$  values at these conditions. When calculating the Gibbs free energy, the entropy, without temperature effects (i.e., at 0 K), is equal to zero for solid materials [77,78].

The results of the free energy calculations are plotted in Fig. 4 near the closest fit range observed in Figs. 2 and 3. Free energies were also calculated from spatial coordinates obtained from additional GCMC simulations at  $T = 280$  K and  $P = 10$  MPa for  $k_{ij} = \{1.06, 1.08\}$  to further examine this range, and are included in Fig. 4. A linear trend fitted to the data shows a slight decrease in the Gibbs free energy with increasing  $k_{ij}$ , relative to the reference case. It should be noted, however, that the uncertainties are large, in relative terms, due to the fact that the absolute difference in  $G$  is less than  $5 \text{ kJ}\cdot\text{mol}^{-1}$  over the range of  $k_{ij}$  values considered in this study. Therefore, it is unclear if the unlike dispersion interactions significantly influence the stability of methane clathrate hydrates under the conditions investigated here.

The results of the free energy analysis also suggests that, at least at  $T = 280$  K and  $P = 10$  MPa, increasing the amount of adsorbed methane does not produce a significantly more thermodynamically stable sI clathrate hydrate. This suggests that clathrate hydrate stability may not be governed solely by the unlike dispersion interaction.

It should be noted that although  $k_{ij} = \{0.80, 0.95\}$  was considered in this study, this parameter range would not be practical for describing the methane clathrate hydrate system. This is due to the fact that decreasing the unlike dispersion interactions would actually result in the simulated system deviating further from reality than it already does, since a polarizability contribution must be added to the unlike interactions. With respect to the fitted adsorption isotherm parameters (see Table 2 and Figs. 2 and 3), however, the trends observed continue even when decreasing  $k_{ij}$  below unity. This must be considered in conjunction with a previous analysis of the relative stability of hydrate structures (i.e., sI, sII or sH) with respect to the unlike dispersion interaction [74]. Should  $k_{ij}$  decrease sufficiently, then the most stable structure for methane clathrate hydrate can become sII (below a value of about  $6.07 \text{ kJ}\cdot\text{mol}^{-1}$

for  $\varepsilon_{ij}$ ), which is at odds with current knowledge of methane clathrate hydrate. Therefore, while the trends may continue monotonically down to a point below  $k_{ij} = 1$ , it would not be desirable to impose such values for unlike dispersion interactions.

### 3.2. Direct estimation of the heat of dissociation

The results of the calculations described in Section 2.4. for the heat of dissociation for various  $k_{ij}$  values are shown in Fig. 5, and are compared to experimental data obtained by calorimetry [79]. There is a monotonic trend for the heat of dissociation in terms of the unlike dispersion, which suggests that fitting to experimental data may be achieved. For methane clathrate hydrates in particular, a value best matching the calorimetric data is in the range  $1.029 < k_{ij} < 1.03$ . It can also be stated that the unlike dispersion produces a large effect on the directly-calculated heat of dissociation. For example, a 3 % change in  $k_{ij}$  results in a 71.7 % change in the heat of dissociation (see Fig. 5). Therefore, there can be limitations on this approach if the experimental data used as a reference possesses large uncertainties.

It can also be stated that the ‘best fit’ range obtained using this alternative approach is again at odds with a value estimated via ionization potentials using the approach of Reed [47], as expanded upon by Hudson and McCoubrey [48]. This serves to emphasize the fact that intermolecular potentials fitted to clathrate hydrate data are not generally applicable.

The decrease in the heat of dissociation with increasing  $k_{ij}$  suggests increasing the unlike dispersion interaction reduces the enthalpy difference between the solid phase and the weighted sum of the fluid phases (gaseous methane and liquid water). It is also apparent that the heat of dissociation becomes increasingly sensitive to changes in the unlike dispersion interaction as  $k_{ij}$  increases, as evidenced by the increasingly negative slope of the curve in Fig. 5 for  $k_{ij} > 1.02$ . In a previous study [69], it was found that increasing  $k_{ij}$  moderately expands the hydrate crystal, and causes the magnitude of the internal energy of the host water lattice to increase. It can also be expected that increasing  $k_{ij}$  increases the internal energy of the combined water-methane clathrate hydrate system. Therefore, since the enthalpy consists (by definition) of internal energy and volume contributions (provided the pressure is constant), it can be expected that increasing the heat of dissociation can be more sensitive to changes in the unlike dispersion interaction than either the internal energy or the cell constant, which was observed in the present study and in the literature [69].

The heat of dissociation from Fig. 5 was then used to compute the phase equilibria via eq. (5), which are shown in Fig. 6. As expected from the calculated heat of dissociation, the phase equilibria show a monotonic trend with respect to  $k_{ij}$ . It is also apparent that the ‘best fit’ value for unlike dispersion interaction obtained by this approach lies in the range  $1.029 < k_{ij} < 1.03$ , which concurs with the value obtained using the heat of dissociation measured by calorimetry. Previously [69], a value of  $k_{ij} = 1.02$  was found to best reproduce the experimental value of the cell constant, which agrees roughly with the value obtained in the present study.

A significant drawback of directly estimating the heat of dissociation, as opposed to employing GCMC simulations to infer phase equilibria of clathrate hydrates, is that the occupancy behaviour cannot be computed. At best, Langmuir adsorption isotherm parameters can be fitted to the phase equilibria estimated via the Clausius-Clapeyron equation, although no details about molecular behaviour can be determined by this approach. Therefore, in order to fully study various aspects of clathrate hydrate systems by computational means, it is necessary to employ a variety of methodologies.

#### **4. Conclusions**

Adsorption isotherm parameters were fitted to the results of GCMC simulations for a range of  $k_{ij}$  values. These parameters change monotonically with respect to unlike dispersion interactions, although a simultaneous fit to both values regressed from experimental phase equilibria is not possible (at least using the force fields considered in this study). The closest fit to experimental data (using GCMC simulations) lies in the range  $1.05 < k_{ij} < 1.07$ .

The heat of dissociation was estimated directly by computing the enthalpies of the fluid phases (pure gaseous methane and pure liquid water), and the enthalpy of the solid phase (the methane clathrate hydrate). The unlike dispersion interaction monotonically influences the calculated heat of dissociation, as well as the phase equilibria estimated via the Clausius-Clapeyron equation. A ‘best fit’ value for  $k_{ij}$  (using direct estimation of the heat of dissociation) was found to be in the range  $1.029 < k_{ij} < 1.03$ .

#### **Acknowledgements**

This work is based on research supported by the South African Research Chairs Initiative of the Department of Science and Technology and National Research Foundation. The authors

would like to thank the NRF Focus Area Programme and the NRF Thuthuka Programme, as well as the Swedish International Development Cooperation Agency. The authors would also like to thank the CSIR Centre for High Performance Computing in Cape Town for the use of their computing resources.

## References

- [1] E.D. Sloan, C.A. Koh, Clathrate Hydrates of Natural Gases, CRC Press, Boca Raton, 2008.
- [2] E.G. Hammerschmidt, *Ind. Eng. Chem.* 26 (1934) 851–855.
- [3] Welling and Associates, 1999 Survey, cited by N. Macintosh, *Flow Assurance Still Leading Concern among Producers, Offshore*, October, 2000.
- [4] S. Thomas, R.A. Dawe, *Energy* 28 (2003) 1461–1477.
- [5] A.A. Khokhar, J.S. Gudmundsson, E.D. Sloan, *Fluid Phase Equilib.* 150 (1998)383–392.
- [6] N.I. Papadimitriou, I.N. Tsimpanogiannis, I.G. Economou, A.K. Stubos, *Mol. Phys.* (2014) in press.
- [7] A.R.C. Duarte, A. Shariati, C.J. Peters, *J. Chem. Eng. Data* 54 (2009) 1628-1632.
- [8] A.T. Trueba, L.J. Rovetto, L.J. Florusse, M.C. Kroon, C.J. Peters, *Fluid Phase Equilibria* 307 (2011) 6-10.
- [9] H.A. Lorentz, *Ann. Phys.* 12 (1881) 127-136.
- [10] D.C. Berthelot, *Compt. Rend.* 126 (1898) 1703-1706.
- [11] J.E. Lennard-Jones, *Proc. Phys. Soc.* 43 (1931) 461-482.
- [12] N.I. Papadimitriou, I.N. Tsimpanogiannis, I.G. Economou, A.K. Stubos, Influence of combining rules on the cavity occupancy of clathrate hydrates: Monte Carlo simulations and van der Waals-Platteeuw-theory-based modeling, *Thermodynamics 2013 conference*, Manchester, United Kingdom, 2013.
- [13] J. Delhommelle, P. Millie, *Mol. Phys.* 99 (2001) 619-625.
- [14] A.J. Haslam, A Galindo, G. Jackson, *Fluid Phase Equilibria* 266 (2008) 105-128.

- [15] E.L. Johansson, Simulations of water clustering in vapour, hydrocarbons and polymers, PhD thesis, Chalmers University of Technology, 2007.
- [16] S. Moodley, E. Johansson, K. Bolton, D. Ramjugernath, *Mol. Sim.* 38 (2012) 838-849.
- [17] D.-M. Duh, A. Henderson, R.L. Rowley, *Mol. Phys.* 91 (1997) 1143-1147.
- [18] H. Doherty, A. Galindo, C. Vega, E. Sanz, *J. Chem. Phys.* 125 (2006) 074510.
- [19] B. Guillot, Y. Guissani, *J. Chem. Phys.* 99 (1993) 8075-8094.
- [20] D. Paschek, *J. Chem. Phys.* 120 (2004) 6674-6690.
- [21] J.H. van der Waals, J.C. Platteeuw, *Adv. Chem. Phys.* 2 (1959) 1-57.
- [22] G.D. Holder, S. Zetts, N. Pradhan, *Rev. Chem. Eng.* 5 (1988) 1-70.
- [23] N.I. Papadimitriou, I.N. Tsimpanogiannis, A.K. Stubos, in *Proceedings of the 7th International Conference on Clathrate Hydrates*, Edinburgh, United Kingdom, 2011.
- [24] W.M. Deaton, E.M. Frost Jr., *Gas Hydrates and Their Relation to the Operation of Natural Gas Pipelines*, U.S. Bureau of Mines Monograph 8, 1946.
- [25] D.R. Marshall, S. Saito, R. Kobayashi, *AIChE J.* 10 (1964) 202-205.
- [26] W.R. Parrish, J.M. Prausnitz, *Ind. Eng. Chem. Process Des. Develop.* 11 (1972) 26-34.
- [27] M. Lasich, A.H. Mohammadi, K. Bolton, J. Vrabec, D. Ramjugernath, *Fluid Phase Equilibria* 369 (2014) 47-54.
- [28] M.M. Conde, C. Vega, *J. Chem. Phys.* 133 (2010) 064507.
- [29] M.M. Conde, C. Vega, *J. Chem. Phys.* 138 (2013) 056101.
- [30] E.K. Karakatsani, G.M. Kontogeorgis, *Ind. Eng. Chem. Res.* 52 (2013) 3499-3513.
- [31] E.D. Sloan, F. Fleyfel, *Fluid Phase Equilibria* 76 (1992) 123-140.
- [32] R.J. Sadus, *Molecular Simulation of Fluids*, Elsevier, Amsterdam, 1999.
- [33] I.N. Tsimpanogiannis, N.I. Diamantonis, I.G. Economou, N.I. Papadimitriou, A.K. Stubos, *Fluid Phase Equilibria* (2014) in press.
- [34] E.D. Sloan Jr., *Clathrate Hydrates of Natural Gases*, 2<sup>nd</sup> ed., revised and expanded, Marcel Dekker, Monticello, NY, 1998.
- [35] V.T. John, G.D. Holder, *J. Phys. Chem.* 85 (1981) 1811-1814.
- [36] G.D. Holder, D.J. Manginello, *Chem. Eng. Sci.* 37 (1982) 9-16.
- [37] V.T. John, G.D. Holder, *J. Phys. Chem.* 86 (1982) 455-459.
- [38] J.S. Tse, D.W. Davidson, in *Proceedings of the 4<sup>th</sup> Canadian Permafrost Conference*, Calgary, Alberta, Canada, 1982.
- [39] V.T. John, G.D. Holder, *J. Phys. Chem.* 89 (1985) 3279-3285.
- [40] V.T. John, K.D. Papadopoulos, G.D. Holder, *AIChE J.* 31 (1985) 252-259.
- [41] D. Avlontis, *Chem. Eng. Sci.* 49 (1994) 1161-1173.

- [42] R.J. Bakker, J. Dubessy, M. Cathelineau, *Geochim. Cosmochim. Acta* 60 (1996) 1657-1681.
- [43] R.J. Bakker, in J.-P. Henriot, J. Mienert (Eds.) *Gas Hydrates: Relevance to World Margin Stability and Climate Change*, Geological Society, London, pp. 75-110.
- [44] K.A. Sparks, J.W. Tester, Z. Cao, B.L. Trout, *J. Phys. Chem. B* 103 (1999) 6300-6308.
- [45] B.J. Anderson, J.W. Tester, B.L. Trout, *J. Phys. Chem. B* 108 (2004) 18705-18715.
- [46] B.J. Anderson, M.Z. Bazant, J.W. Tester, B.L. Trout, *J. Phys. Chem. B* 109 (2005) 8153-8163.
- [47] T.M. Reed III, *J. Phys. Chem.* 59 (1955) 425-432.
- [48] G.H. Hudson, J.C. McCoubrey, *Trans. Faraday Soc.* 56 (1960) 761-766.
- [49] I.N. Tsimpanogiannis, N.I. Papadimitriou, A.K. Stubos, *Mol. Phys.* 110 (2012) 1213-1221.
- [50] J.J. Potoff, A.Z. Panagiotopoulos, *J. Chem. Phys.* 109 (1998) 10914-10920.
- [51] J.M. Smith, H.C. Van Ness, M.M. Abbott, *Introduction to Chemical Engineering Thermodynamics*, 7<sup>th</sup> ed., McGraw-Hill, New York, 2005.
- [52] H.J.C. Berendsen, P.J.M. Postma, W.F. van Gunsteren, J. Hermans, In: B. Pullman (Ed.), *Intermolecular Forces*, Reidel, Dordrecht, 1981, pp. 331-342.
- [53] S.R. Zele, S.-Y. Lee, G.D. Holder, *J. Phys. Chem. B* 103 (1999) 10250-10257.
- [54] R. Shevchuk, D. Prada-Garcia, F. Rao, *J. Phys. Chem. B* 116 (2012) 7538-7543.
- [55] P.P. Ewald, *Ann. Phys.* 64 (1921) 253-287.
- [56] J.D. Gale, A.L. Rohl, *Mol. Sim.* 29 (2003) 291-341.
- [57] M.P. Allen, D.J. Tildesley, *Computer Simulations of Liquids*, Clarendon Press, Oxford, 1987.
- [58] D. Frenkel, B. Smit, *Understanding Molecular Simulation*, Academic Press, San Diego, 2002.
- [59] Metropolis, A.W. Rosenbluth, M.N. Rosenbluth, A.H. Teller, E. Teller, *J. Chem. Phys.* 21 (1953) 1087-1092.
- [60] J. Vrabec, H. Hasse, *Molecular Physics* 100 (2002) 3375-3383.
- [61] S. Deublein, B. Eckl, J. Stoll, S.V. Lishchuk, G. Guevara-Carrion, C.W. Glass, T. Merker, M. Bernreuther, H. Hasse, J. Vrabec, *Computer Physics Communications* 182 (2011) 2350-2367.
- [62] B. Widom, *J. Chem. Phys.* 39 (1963) 2808-2812.
- [63] N.I. Papadimitriou, I.N. Tsimpanogiannis, A.Th. Papaioannou, A.K. Stubos, *J. Phys. Chem. C* 112 (2008) 10294-10302.

- [64] N.I. Papadimitriou, I.N. Tsimpanogiannis, A.Th. Papaioannou, A.K. Stubos, *Mol. Sim.* 34 (2008) 1311-1320.
- [65] A. Lenz, L. Ojamäe, *J. Phys. Chem. A* 115 (2011) 6169-6169.
- [66] P. Atkins, J. de Paula, *Atkins' Physical Chemistry*, 7<sup>th</sup> ed., Oxford University Press, New York, 2002.
- [67] I. Langmuir, *J. Am. Chem. Soc.* 40 (1918) 1361-1368.
- [68] L. Jensen, *Experimental Investigation and Molecular Simulation of Gas Hydrates* (Ph.D. Thesis), Technical University of Denmark, 2010.
- [69] M. Lasich, A.H. Mohammadi, K. Bolton, J. Vrabec, D. Ramjugernath, *Phil. Mag.* 94 (2014) 974-990.
- [70] J.M. Sneddon, J.D. Gale, *Thermodynamics and Statistical Mechanics*, Royal Society of Chemistry, London, 2002.
- [71] H.J. Monkhorst, J.D. Pack, *Phys. Rev. B* 13 (1976) 5188-5192.
- [72] W. Cochran, R.A. Cowley, *J. Phys. Chem. Solids* 23 (1962) 447-450.
- [73] S. Baroni, S. de Gironcoli, A. Dal Corso, P. Giannozzi, *Rev. Mod. Phys.* 73 (2001) 515-562.
- [74] L.C. Jacobson, V. Molinero, *J. Phys. Chem. B* 114 (2010) 7302-7311.
- [75] J. Berkowitz, J.P. Greene, H. Cho, B. Ruscic, *J. Chem. Phys.* 86 (1987) 674-676.
- [76] K.B. Snow, T.F. Thomas, *Int. J. Mass. Spectrom. Ion Processes*, 96 (1990) 49-68.
- [77] T. Miyoshi, M. Imai, R. Ohmura, K. Yasuoka, *J. Chem. Phys.* 126 (2007) 234506.
- [78] C. Wolverton, A. Zunger, *Phys. Rev. B* 57 (1998) 2242-2252.
- [79] M. K. Aydinol, A. F. Kohn, G. Ceder, K. Cho, J. Joannopoulos, *Phys. Rev. B* 56 (1997) 1354-1365.
- [80] A. Gupta, J. Lachance, E.D. Sloan Jr., C.A. Koh, *Chem. Eng. Sci.* 63 (2008) 5848-5853.

Force field	Non-bonded interactions (Lennard-Jones [11])	Charges	Bond angle	Bond length
United atom LJ methane [34,35]	$\varepsilon_{CH_4} / k_B = 145.27$ K $\sigma_{CH_4} = 0.3821$ nm			
SPC water [36]	$\varepsilon_O / k_B = 78.21$ K $\sigma_O = 0.3166$ nm	$q_O = -0.82$ e $q_H = +0.41$ e	$\alpha_{(H-O-H)} = 109.47^\circ$	$r_{O-H} = 0.1$ nm

**Table 1.** Force field parameters used in this study.

$k_{ij}$	$A / \text{K.MPa}^{-1}$	$B / 10^3 \text{ K}$	AAD / %
1.25	279	0.564	7.9
1.10	67.0	1.00	4.2
1.07	58.8	0.993	7.5
1.05	27.1	1.31	7.9
1 [27]	19.1	1.31	6.3
0.95	12.2	1.45	8.5
0.85	11.2	1.50	6.8
0.80	9.92	1.50	8.0

**Table 2.** Fitted adsorption isotherm parameters obtained from GCMC simulations; see eq. (3). AAD is the absolute average deviation of fitted adsorption isotherms to GCMC simulation results.

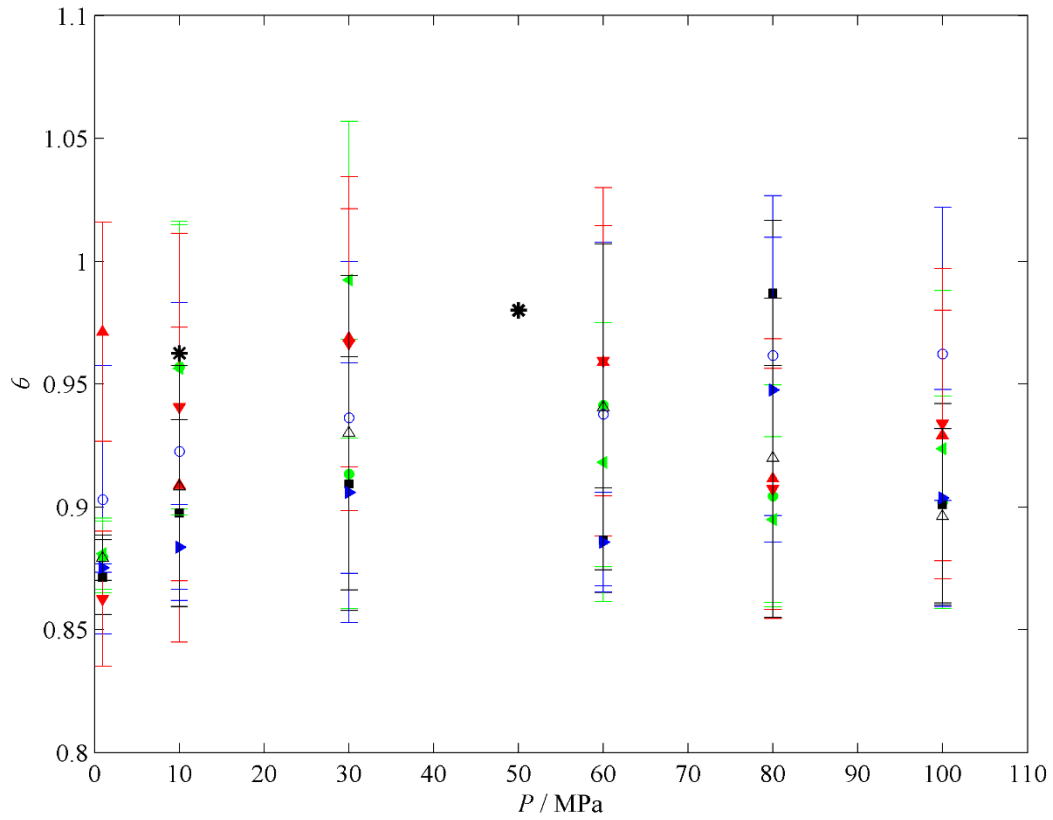


**Fig. 1.** Plot of overall fractional occupancy  $\theta$  (see eq. (6)) versus pressure  $P$  for sI methane clathrate hydrate at  $T = 273.2$  K. ( $\bullet$ )  $k_{ij} = 0.80$ , ( $\circ$ )  $k_{ij} = 0.85$ , ( $\blacktriangle$ )  $k_{ij} = 0.95$ , ( $\blacksquare$ )  $k_{ij} = 1$  [27], ( $\blacktriangleleft$ )  $k_{ij} = 1.05$ , ( $\blacktriangleright$ )  $k_{ij} = 1.07$ , ( $\blacktriangledown$ )  $k_{ij} = 1.10$ , ( $\triangle$ )  $k_{ij} = 1.25$ . (\*) simulated adsorption data obtained by Papadimitriou and co-workers [23] at  $T = 273$  K.

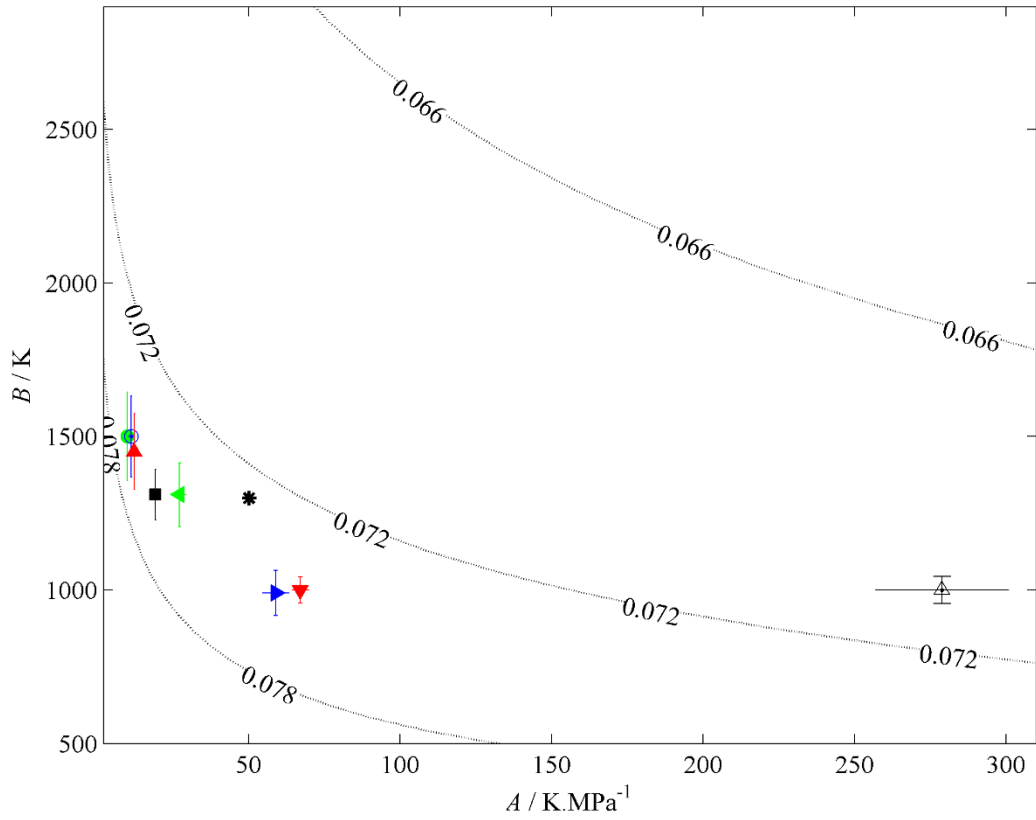


**Fig. 2.** Plot of the solution space for the slope of the dissociation pressure curve; see eq. (11). (···) lines of constant slope (in  $\text{K}^{-1}$ ), (\*) adsorption isotherm parameters fitted to experimental data [24,25]. Adsorption isotherm parameters fitted to GCMC results: (●)  $k_{ij} = 0.80$ , (○)  $k_{ij} = 0.85$ , (▲)  $k_{ij} = 0.95$ , (■)  $k_{ij} = 1$  [27], (▼)  $k_{ij} = 1.05$ , (▶)  $k_{ij} = 1.07$ , (▼)  $k_{ij} = 1.10$ , (Δ)  $k_{ij} = 1.25$ .

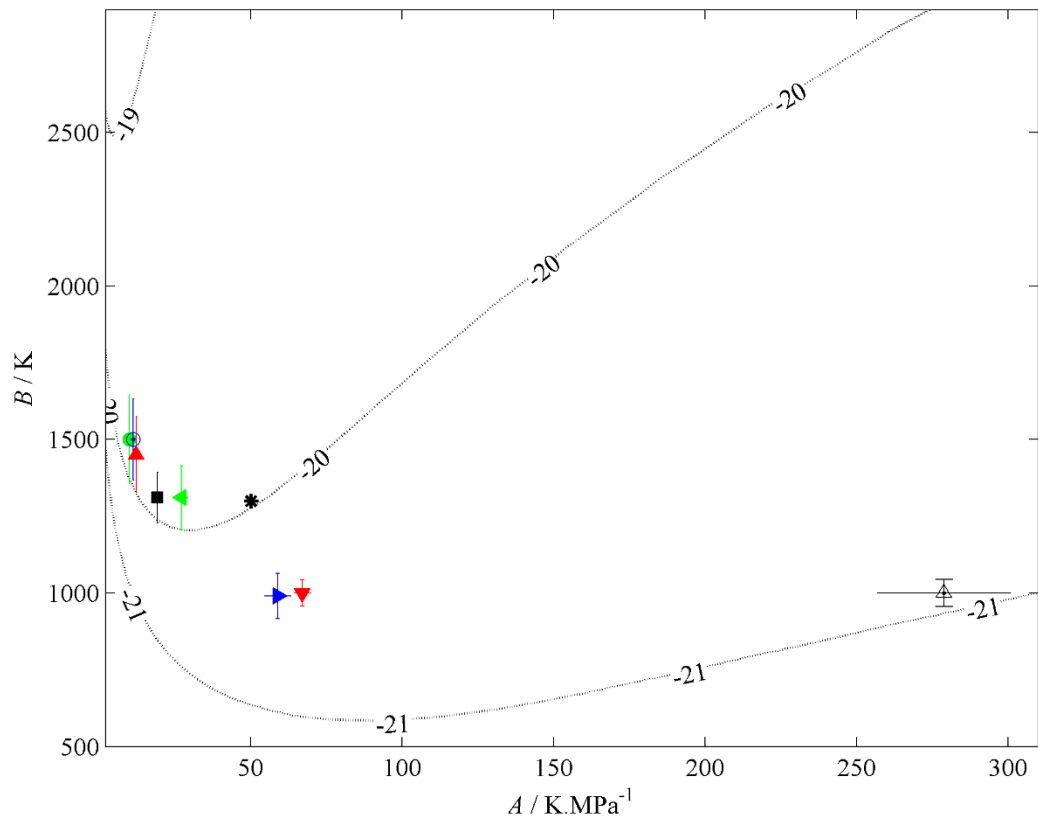


**Fig. 3.** Plot of the solution space for the intercept of the dissociation pressure curve; see eq. (11). (···) lines of constant intercept (dimensionless), (\*) adsorption isotherm parameters fitted to experimental data [24,25]. Adsorption isotherm parameters fitted to GCMC results: (●)  $k_{ij} = 0.80$ , (○)  $k_{ij} = 0.85$ , (▲)  $k_{ij} = 0.95$ , (■)  $k_{ij} = 1$  [27], (◀)  $k_{ij} = 1.05$ , (▶)  $k_{ij} = 1.07$ , (▼)  $k_{ij} = 1.10$ , (△)  $k_{ij} = 1.25$

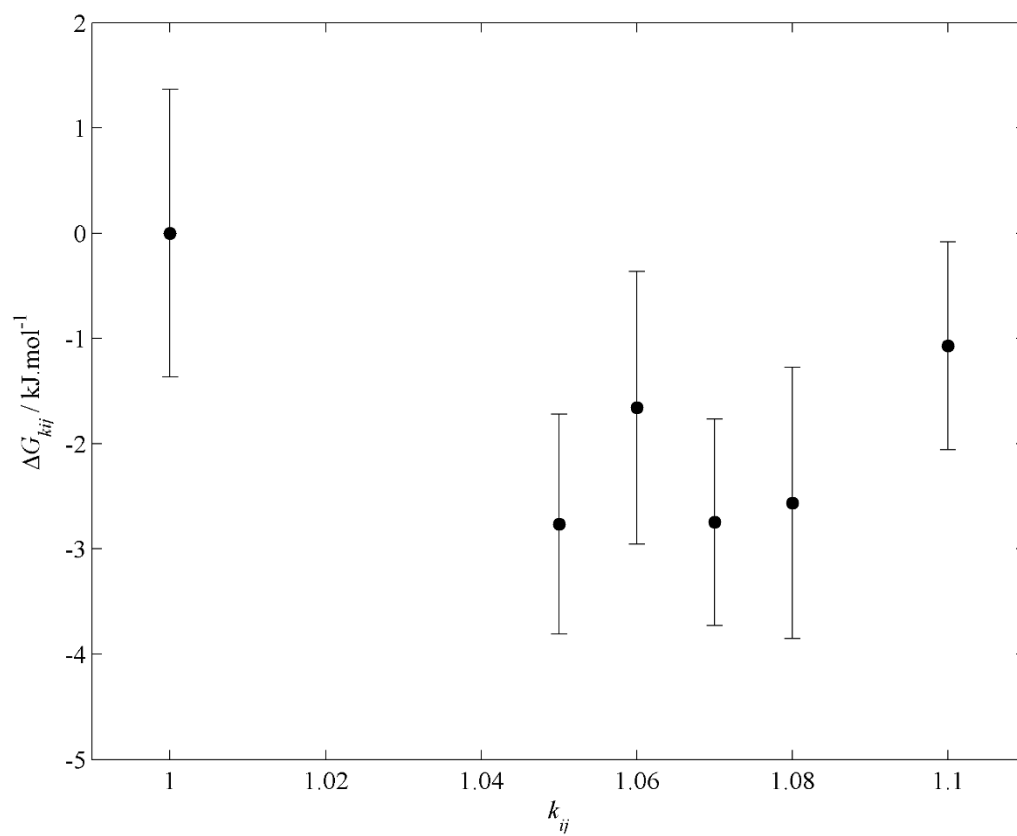


**Fig. 4.** Gibbs free energy of the sI methane clathrate hydrate relative to the reference case (i.e.,  $k_{ij} = 1$ ) for different  $k_{ij}$  values, at  $T = 280$  K and  $P = 10$  MPa.

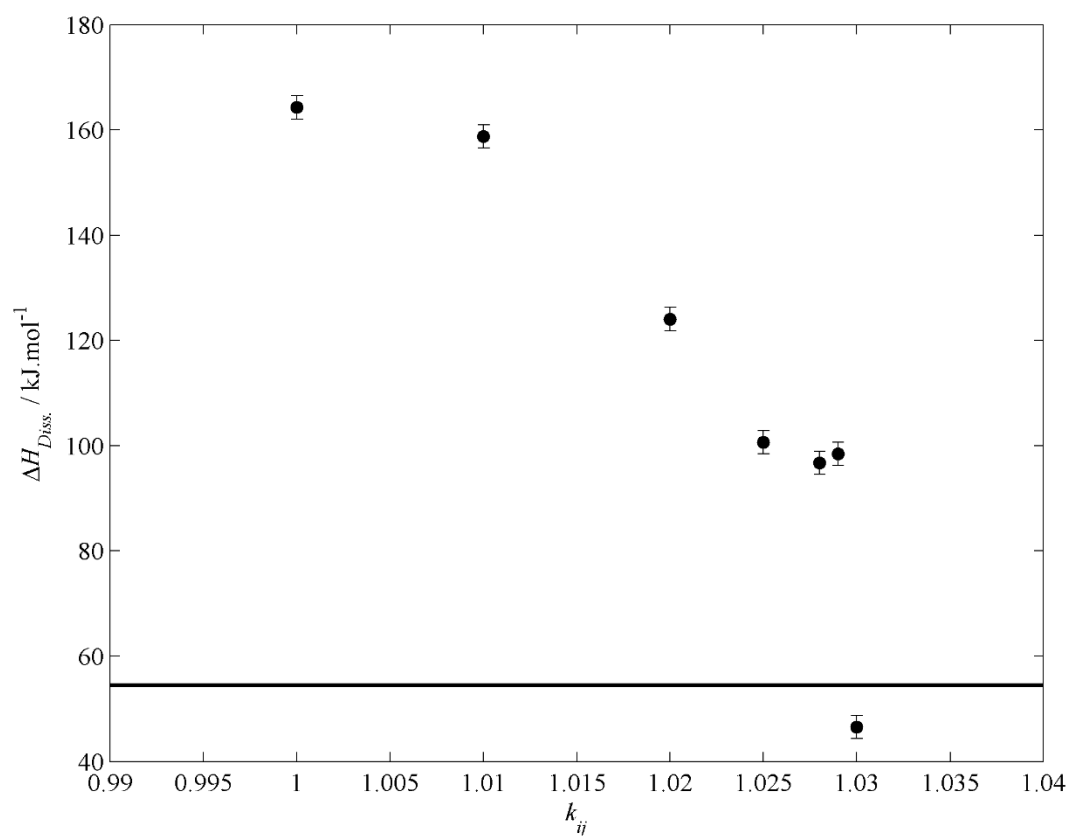


**Fig. 5.** Heat of dissociation as a function of  $k_{ij}$  for methane clathrate hydrate. The solid line corresponds to a literature value of about  $54.4 \text{ kJ.mol}^{-1}$  obtained by calorimetry [79].

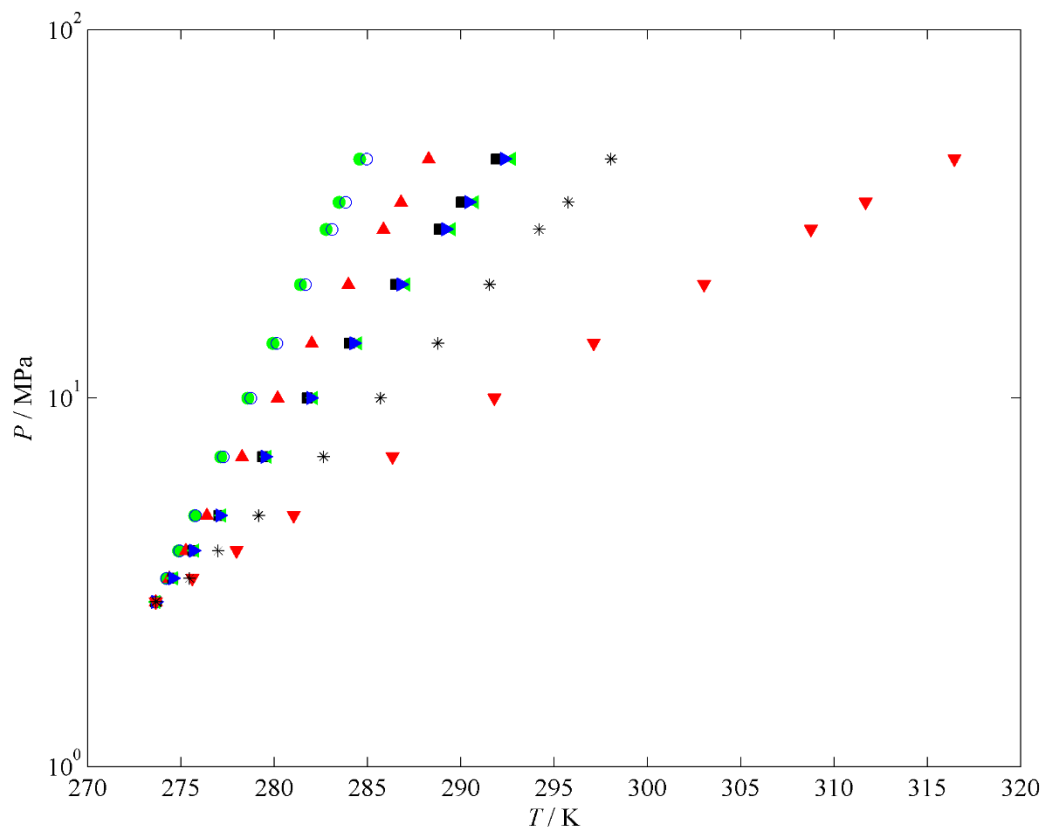


**Fig. 6.** Phase equilibria of methane clathrate hydrate, estimated by computing the enthalpy of the fluid phases and the solid phase, for various  $k_{ij}$  values: (●)  $k_{ij} = 1$ , (○)  $k_{ij} = 1.01$ , (▲)  $k_{ij} = 1.02$ , (■)  $k_{ij} = 1.025$ , (◀)  $k_{ij} = 1.028$ , (▶)  $k_{ij} = 1.029$ , (▼)  $k_{ij} = 1.03$ . (\*) experimental data [24,25].

## Supplementary material

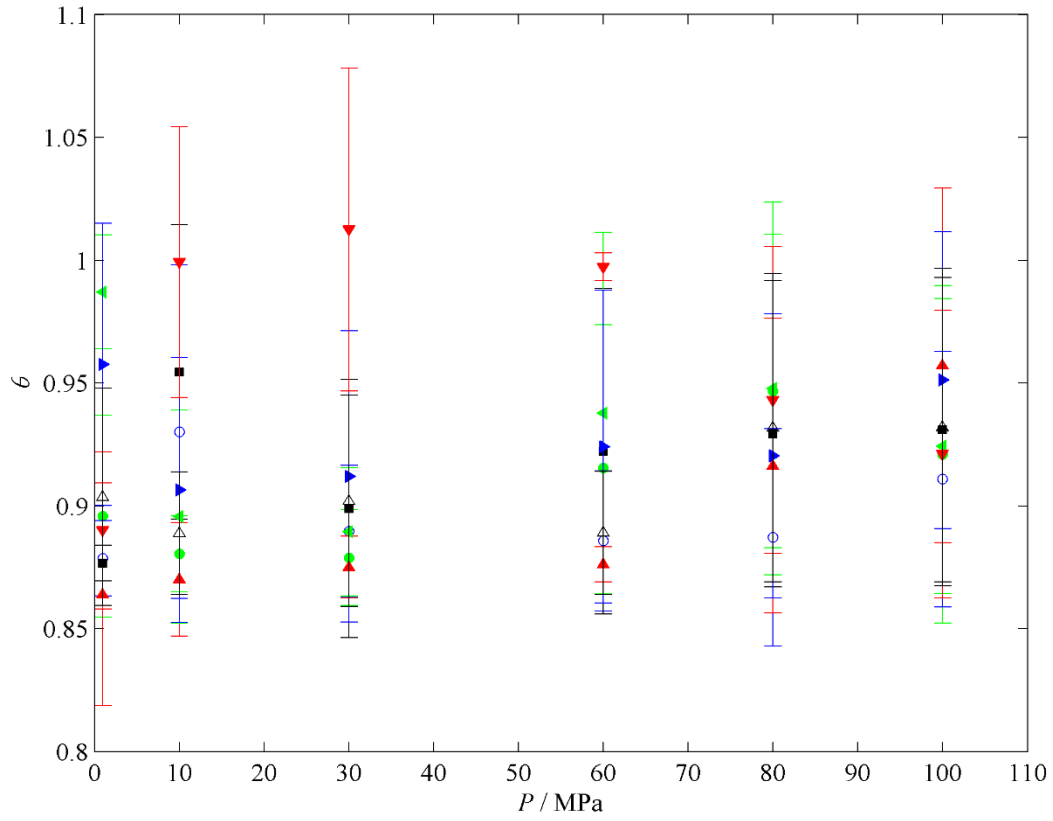


**Fig. A1.** Plot of overall fractional occupancy  $\theta$  (see eq. (6)) versus pressure  $P$  for sI methane clathrate hydrate at  $T = 280$  K. ( $\bullet$ )  $k_{ij} = 0.80$ , ( $\circ$ )  $k_{ij} = 0.85$ , ( $\blacktriangle$ )  $k_{ij} = 0.95$ , ( $\blacksquare$ )  $k_{ij} = 1$  [27], ( $\blacktriangleleft$ )  $k_{ij} = 1.05$ , ( $\blacktriangleright$ )  $k_{ij} = 1.07$ , ( $\blacktriangledown$ )  $k_{ij} = 1.10$ , ( $\triangle$ )  $k_{ij} = 1.25$ . (\*) simulated adsorption data obtained by Papadimitriou and co-workers [23] at  $T = 273$  K.

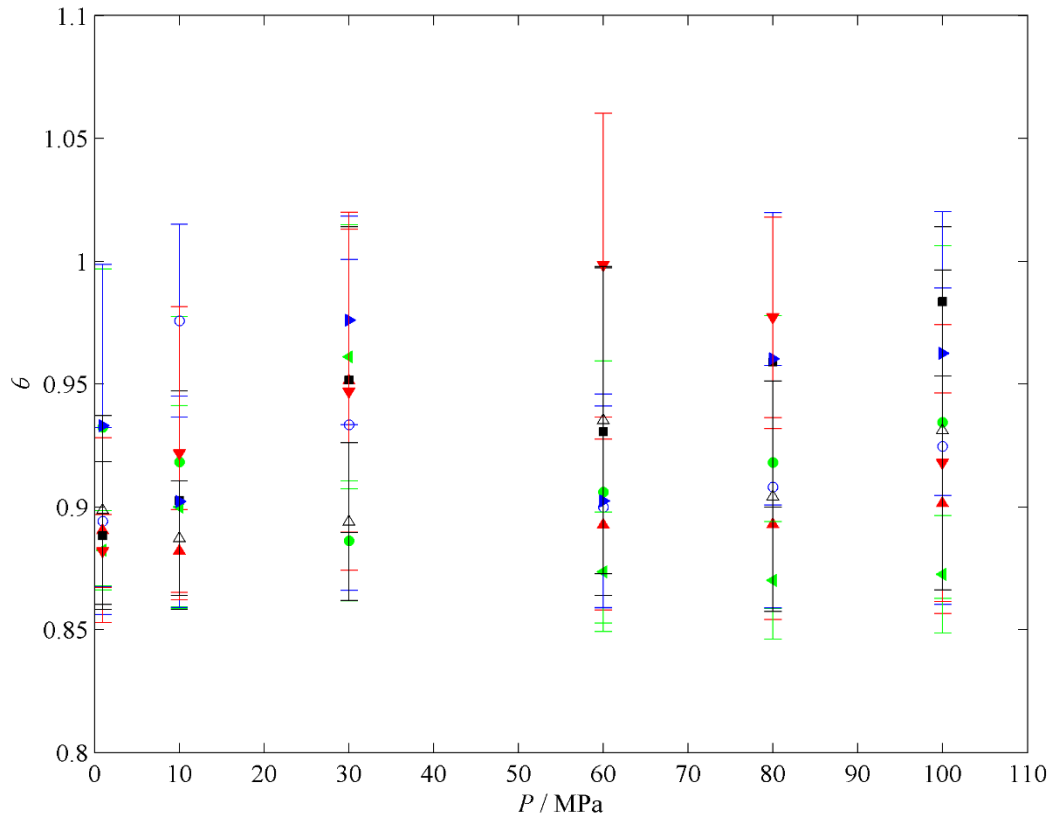


**Fig. A2.** Plot of overall fractional occupancy  $\theta$  (see eq. (6)) versus pressure  $P$  for sI methane clathrate hydrate at  $T = 300$  K. ( $\bullet$ )  $k_{ij} = 0.80$ , ( $\circ$ )  $k_{ij} = 0.85$ , ( $\blacktriangle$ )  $k_{ij} = 0.95$ , ( $\blacksquare$ )  $k_{ij} = 1$  [27], ( $\blacktriangleleft$ )  $k_{ij} = 1.05$ , ( $\blacktriangleright$ )  $k_{ij} = 1.07$ , ( $\blacktriangledown$ )  $k_{ij} = 1.10$ , ( $\triangle$ )  $k_{ij} = 1.25$ . (\*) simulated adsorption data obtained by Papadimitriou and co-workers [23] at  $T = 273$  K.